Supporting Information

Ultrafine Pd Nanoparticles Loaded Benzothiazole-linked Covalent Organic Framework for Efficient Photocatalytic Cross-Coupling Reactions

Yongliang Yang[a,b], Hongyun Niu[a] , Weijia Zhao[a,b], Lin Xu[a], Hui Zhang[a] and Yaqi Cai[a,c,d]*

[a] State Key Laboratory of Environmental Chemistry and Ecotoxicology
Research Center for Eco-Environmental Sciences, Chinese Academy of Sciences, Beijing, 100085, China
E-mail: caiyaqi@rcees.ac.cn (Y. Cai).
[b] University of Chinese Academy of Sciences
Beijing, 100049, China
[c] Institute of Environment and Health, Jianghan University, Wuhan 430056, China.
[d] Institute of Environment and Health, Hangzhou Institute for Advanced Study, UCAS

Section S1 General Information

Materials

4,4',4''-(1,3,5-triazine-2,4,6-triyl)trianiline, trifluoromethanesulfonic acid, 4-bromobenzotitrile, 4-cyanophenylhydrazine, butyl lithium, 1,4-dioxane, mesitylene, potassium carbonates, sodium tetrachloropalladate(II) and tributylphenylstannane were purchased from J&K Chemical Co. Ltd. (Beijing, China). Acetone, methanol, ethanol, tetrahydrofuran (THF), sulfur, acetic acid (≥99.5%) were obtained from Sinopharm Chemistry Reagent Co. Ltd. (Beijing, China). Iodobenzene, 4-iodotoluene, 4-iodoanisole, 1-iodo-4-nitrobenzene, phenylboronic acid, styrene, ethynylbenzene and *trans*-stilbene were purchased from Tokyo Chemical Industry (TCI). 4,4',4''-(1,3,5-triazine-2,4,6-triyl)tribenzaldehyde were synthesized following published procedures.[1]

Characterization

Powder X-ray diffraction (PXRD, Almelo, Netherlands) using a Cu Ka radiation ranging from 3º to 60º with a resolution of 0.02° was utilized to analysis the crystalline. The microstructures of the catalysts were investigated by field emission scanning electron microscope (FE-SEM, Quattro ESEM, Thermo Fisher) and high-resolution transmission electron microscope (HR-TEM, JEM-2100F, JEOL) at accelerating voltage of 200 kV. Surface analysis by X-ray photoelectron spectroscopy (XPS) was carried out using Thermo Fisher ESCALAB 250Xi equipment (Waltham, MA), and the X-ray source was Al Kα radiation (1486.6 eV, monochromatic). Fourier transform-infrared (FT-IR) spectra in the 4000–400 cm^{-1} region were recorded on a NEXUS 670 Infrared Fourier Transform Spectrometer (Nicolet Thermo, Waltham, MA). Solid-state nuclear magnetic resonance (ssNMR) spectroscopy was obtained on a JNM-ECZ600R spectrometer (JEOL). Pd element analysis was carried out on the NexION 300 inductively coupled plasma mass spectrometry (ICP-MS) (Perkin Elmer, U.S.A.). Elemental analysis (EA) was conducted on an EA3000 analyzer (EUROVECTOR). Thermogravimetric analysis (TGA) was carried out on a TGA Q5000 IR thermogravimetric analyzer (TA Instruments, New Castle, U.S.A.) with the heating rate of 10 °C min^{-1} under N_2 atmosphere. Surface area and pore volume were measured by Brunauer Emmett-Teller (BET) methods (ASAP2000 V3.01A; Micrometritics, Norcross, GA). The diffuse reflectance spectra (DRS) were collected using a Hitachi U-3900 UV–vis spectrophotometer ($BaSO_4$ as a reflectance standard). All contact angles were measured on the OCA20 Contact Angle Measuring System (Dataphysics). The photoluminescence (PL) spectra of samples were detected on an FS5 fluorescence spectrometer (Edinburgh Instruments, England). All the electrochemical properties were investigated on a CHI852D electrochemical analyzer (Chenhua, Shanghai, China) in a standard three-electrode system, using a platinum foil as the counter electrode and Ag/AgCl (saturated KCl) as the reference electrode. The electrolyte was a 0.1 $mol.L^{-1}$ Na_2SO_4 aqueous solution. The working electrodes were prepared as follows: 5 mg of photocatalyst powder was dispersed in 0.5 mL of DMF, which was dip-coated on the surface of indium tin oxide (ITO) glass substrate. Subsequently, 5% Nafion-ethanol solution was dripped onto the sample film and dried at 100 °C. Mott-Schottky curves were measured at a frequency of 1 kHz. The EIS frequency ranged from 10 m to 100

kHz with an AC voltage magnitude of 10 mV. Visible-light irradiation was provided by a CEL-HXF300F3 300 W xenon lamp (CEAULIGHT) with a 420 nm cut-off filter. Gas chromatography-Mass spectrometer (GC-MS) analysis was carried out on an Agilent 7890A/5975C. Nuclear magnetic resonance (NMR) spectra were recorded on a Bruker Avance 400 spectrometer at ambient temperature. Chemical shifts for ^{1}H NMR spectra are reported in parts per million (ppm) from tetramethylsilane with the solvent resonance as the internal standard (chloroform: δ 7.26 ppm). Chemical shifts for ^{13}C NMR spectra are reported in parts per million (ppm) from tetramethylsilane with the solvent as the internal standard ($CDCl_3$: δ 77.16 ppm). Data are reported as following: chemical shift, multiplicity (s = singlet, d = doublet, dd = doublet of doublets, t = triplet, q = quartet, m = multiplet, br = broad signal), coupling constant (Hz), and integration.

Synthesis of TTI-COF

A quartz tube measuring 10×8 mm (o.d × i.d) was charged 4,4′,4″-(1,3,5-Triazine-2,4,6-triyl)tribenzaldehyde (25.2 mg, 0.064 mmol), 4,4′,4″-(1,3,5-triazine-2,4,6-triyl)trianiline (22.7 mg, 0.064 mmol), mesitylene(1.0 mL), 1,4-dioxane (1.0 mL) and 6 M aqueous acetic acid(100 μL). The tube was sonicated for 15 min, then flash frozen at 77 K in liquid N_2 bath, degassed by one freeze-pump-thaw cycle and flame sealed. The reaction was heated at 120 ºC for 3 days yielding yellow precipitate which was isolated by centrifugation, washed with acetone (15 ml×3) and THF (15 ml×3) and evacuated under vacuum at 120 °C for 10 h to yield activated TTI-COF. Calcd for $[C_{45}N_9H_{27}]_n$: C, 77.91; N, 18.17; H, 3.92%. Found: C, 76.85; N, 18.37; H, 3.79%.

Synthesis of TTT-COF

The activated TTI-COF (100 mg) mixed with sulfur (1 g) in a ball mill. The resulting mixture was transferred to a quartz tube measuring 22×20 mm (o.d × i.d) and flame sealed under vacuum. The tube was heated at 155°C for 3 hours and then raised to 350°C, kept for 3 hours yielding brown powder. The mixture was washed with toluene (10 ml×5) and THF(10 ml×3), and evacuated under vacuum at 150 °C for 10 h to yield TTT-COF. Calcd for $[C_{45}N_9H_{27}S_3]_n$: C, 68.95; N, 16.08; H, 2.70; S, 12.27%. Found: C, 72.15; N, 12.08; H, 1.41; S, 14.36 %.

Synthesis of Pd NPs@COF

In a typical procedure, activated TTT-COF or TTI-COF (100 mg) was dispersed in 5 mL of MeOH under ambient conditions, to which a MeOH solution (2 mL) containing Na_2PdCl_4 (20 mg, 0.07 mmol) was added dropwise under vigorous stirring. The mixture was evaporated until it became mushy. To this solution, 4 mL of MeOH was subsequently added into the slurry, followed by a solution (3 mL) of $NaBH_4$ (2 M in MeOH) under vigorous stirring. After 24 hours of aging, the residue was recovered by filtration and thoroughly washed several times with MeOH (3×10 mL) to remove any impurity.

General procedure for determination of the weight percentage loading of Pd

2 mg Pd NPs@TTT-COF was dissolved in 10 mL aqua regia with sonication for 30 min. After the complete digesting of solid, the solution was filtered through syringe filters (0.22 μm) and diluted 1000 times with 1% HNO_3. ICP-MS was used to detect the content of Pd in Pd NPs@TTT-COF.

General procedure for photocatalytic reaction

A 50 mL quartz reactor was used as the reaction container. After the reactants and catalysts are added into the reactor, the reactor was covered with quartz sheets, then degassed and saturated with N_2 for 30 min to remove the dissolved O_2 before the photocatalytic reactions. The reactions were performed under the irradiation of a 300 W Xe lamp equipped with an optical cutoff filter ($\lambda \geq 420$ nm). The temperature of the reaction systems were kept at room temperature by condenser. After the reaction, the solution was extracted with diethyl ether (5 mL×2) and analyzed by GC-MS and the quantitative analysis of specific analytes was detected by SIM mode in GC-MS. The photocatalysts were recovered, washed with methanol by centrifugation three times, and vacuum dried at 100 °C for 10 h.

Suzuki-Miyaura Cross-Coupling Reactions

Aryl iodide (0.3 or 0.35 mmol) was added to 3 mL ethanol, phenylboronic acid (0.35 or 0.3 mmol) and K_2CO_3 (0.6 mmol) were dissolved in 3 mL H_2O. Ethanol and H_2O solutions were mixed and added to the reactor with sonicating for 15 min. The reaction time was 45 min.

Stille Cross-Coupling Reactions

Aryl iodide (0.3 mmol) and tributylphenylstannane (0.35 mmol) was added to 3 mL ethanol, K_2CO_3 (0.6 mmol) were dissolved in 3 mL H_2O. Ethanol and H_2O solutions were mixed and added to the reactor with sonicating for 15 min. The reaction time was 5 hours.

Heck Cross-Coupling Reactions

Aryl iodide (0.3 mmol) and styrene (0.35 mmol) was added to 3 mL ethanol, K_2CO_3 (0.6 mmol) were dissolved in 3 mL H_2O. Ethanol and H_2O solutions were mixed and added to the reactor with sonicating for 15 min. The reaction time was 5 hours.

Sonogashira Cross-Coupling Reactions

Aryl iodide (0.3 or 0.35 mmol) and ethynylbenzene (0.35 or 0.3 mmol) was added to 3 mL ethanol, K_2CO_3 (0.6 mmol) were dissolved in 3 mL H_2O. Ethanol and H_2O solutions were mixed and added to the reactor with sonicating for 15 min. The reaction time was 5 hours.

Calculation of TOF

$$\mathbf{TOF} = \frac{[\mathbf{amount\ of\ product\ (mol)} \cdot \mathbf{yield}\ (\%)]}{\left[\frac{\mathbf{mass\ of\ Pd}}{\mathbf{Mw\ of\ Pd}\ \left(\frac{\mathbf{g}}{\mathbf{mol}}\right)} \cdot \mathbf{reaction\ time\ (h)}\right]}$$

Section S2 Structure Modeling and PXRD Refinement of TTI-COF and TTT-COF

Structural modeling of TTO-COF was generated using the Accelrys Materials Studio 7.0 software package. The space groups were obtained from the Reticular Chemistry Structure Resource. The model was constructed in the initial lattice with the space group of P1. The proposed model was geometry optimized using the MS Forcite molecular dynamics module (Universal force fields, Ewald summations) to obtain the optimized

lattice parameters. P6 was suitable for AA stacking model of TTI-COF and TTT-COF. AB stacking of TTO-COF was examined by offsetting the stacked units from the AA model. Pawley refinement was applied to define the lattice parameters by Reflex module, producing the refined PXRD profiles. The simulated PXRD patterns of AA stacking are the best agreement with the experimental patterns of both TTI-COF and TTT-COF.

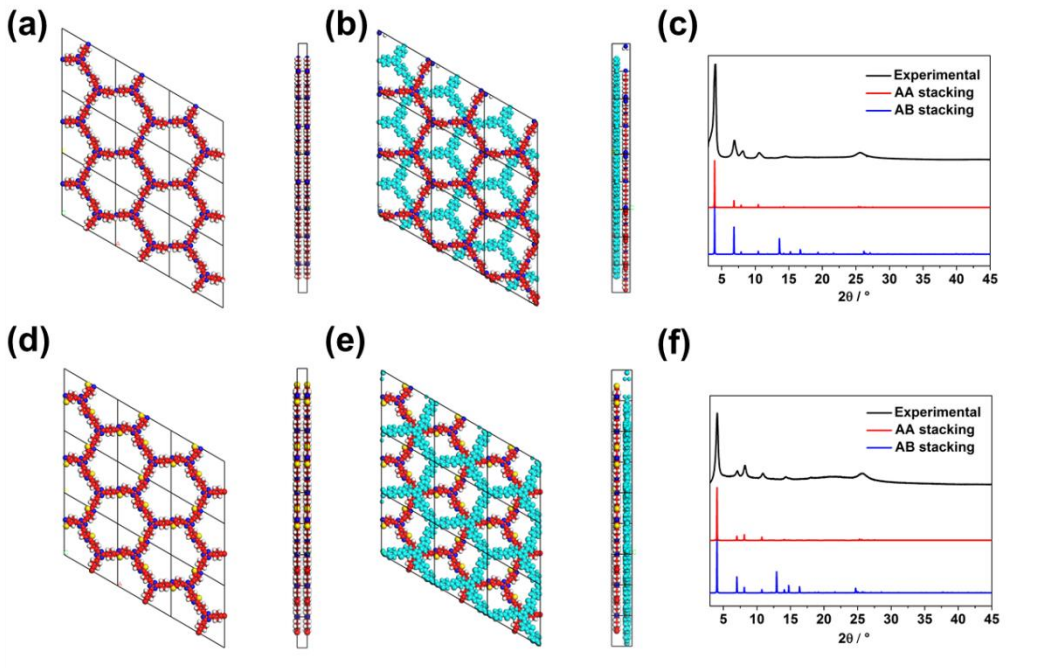

Figure S1. The simulated model of TTI-COF and TTT-COF as well as the comparison of PXRD patterns. The view of the simulated eclipsed AA-stacking (a), staggered AB-stacking (b) model of TTI-COF and eclipsed AA-stacking (d), staggered AB-stacking (e) model of TTT-COF. Simulated PXRD patterns of AA (red) and AB (blue) stacking model compared to experimental pattern (black) of TTI-COF (c) and TTT-COF (f).

Table S1. Atomistic coordinates for the Pawley-refined TTI-COF

TTI-COF	**Hexagonal, P-6** **a = b = 25.54 Å, c = 3.51 Å** **α = β = 90°, γ = 120°**		
Atom	x	y	z
C	-1.29172	13.92539	0
N	-0.06743	13.3346	0
C	-0.26141	17.4622	0
C	0.91423	18.2545	0
C	0.84795	19.65927	0
C	-0.39397	20.3235	0
C	-1.57356	19.54603	0
C	-1.50614	18.14103	0

N	6.05174	11.36402	0
C	7.34397	11.76371	0
C	8.40889	10.84025	0
C	8.19652	9.44167	0
C	9.27983	8.54475	0
C	10.61944	9.00659	0
C	10.82543	10.40871	0
C	9.74301	11.30674	0
C	11.70798	8.1037	0
N	12.99524	8.54121	0
H	1.84059	17.82053	0
H	1.72004	20.1961	0
H	-2.49379	19.98796	0
H	-2.38729	17.62124	0
H	7.55813	12.76327	0
H	7.24922	9.05548	0
H	9.06976	7.54343	0
H	11.77018	10.80066	0
H	9.94351	12.31093	0
C	1.35647	14.03754	0
C	-0.06475	16.27486	0
N	1.25596	15.3932	0
N	-1.18854	15.50999	0
C	-4.67906	13.02361	0
C	3.83111	11.55491	0
C	-3.37022	10.98314	0
C	4.94379	13.70863	0
C	-4.63334	11.61596	0
C	5.0273	12.29833	0
C	-3.49563	13.78339	0
C	2.5814	12.1999	0
C	-2.22166	13.16141	0
C	2.48307	13.61418	0
C	-2.18718	11.74403	0
C	3.69331	14.35273	0
N	-0.09705	21.67784	0
N	-5.95469	11.19592	0
C	11.68104	0.47821	0
C	19.28604	9.87697	0
C	11.94832	1.86219	0
C	17.95384	9.41646	0

C	13.26571	2.37756	0
C	16.84882	10.29966	0
C	13.50081	3.76419	0
C	15.53041	9.80995	0
C	12.43104	4.69341	0
C	15.26057	8.41889	0
C	11.11378	4.17074	0
C	16.37184	7.53945	0
C	10.87727	2.78433	0
C	17.69077	8.02783	0
C	12.6687	6.08756	0
C	13.93437	7.92763	0
N	11.64618	6.9836	0
N	13.66964	6.59408	0
H	-3.58298	14.80263	0
H	1.74239	11.61463	0
H	-5.58	13.51044	0
H	3.85997	10.53125	0
H	-3.29283	9.96523	0
H	5.78663	14.2846	0
H	-1.29645	11.24082	0
H	3.68374	15.37573	0
H	10.70832	0.1639	0
H	20.0446	9.19173	0
H	14.07382	1.75027	0
H	16.98801	11.31315	0
H	14.47302	4.08293	0
H	14.76827	10.49254	0
H	10.30197	4.79294	0
H	16.2389	6.5253	0
H	9.90737	2.45586	0
H	18.46018	7.3521	0

Table S2. Atomistic coordinates for the Pawley-refined TTT-COF

TTT-COF	**Hexagonal, P-6** **a = b = 24.88 Å, c = 3.51 Å** **α = β = 90°, γ = 120°**		
Atom	x	y	z
C	-1.49862	13.87703	0
N	-0.51306	12.9427	0

C	0.49141	17.01746	0
C	1.84796	17.42386	0
C	2.18499	18.78506	0
C	1.16036	19.72801	0
C	-0.15775	19.34898	0
C	-0.52065	18.00286	0
C	7.40007	9.56869	0
C	7.48205	8.16568	0
C	8.72265	7.52398	0
C	9.91324	8.26998	0
C	9.83275	9.67298	0
C	8.59202	10.31447	0
C	11.22973	7.58992	0
N	12.37753	8.31566	0
S	5.88328	11.95579	0
C	6.07636	10.23797	0
N	4.92683	9.52645	0
H	2.6458	16.69273	0
H	3.22243	19.09428	0
H	-1.56916	17.73394	0
H	6.58581	7.55846	0
H	8.74617	6.44161	0
H	10.72949	10.27978	0
H	8.57436	11.39576	0
C	-3.57264	14.43664	0
C	1.72468	11.23587	0
C	-2.54241	13.46503	0
C	2.051	12.61388	0
N	1.48867	14.63251	0
N	-0.97561	15.52116	0
C	1.1723	13.31182	0
C	0.32632	15.90752	0
C	-4.91998	14.04791	0
C	2.735	10.2634	0
C	-5.22429	12.68908	0
C	4.06393	10.67928	0
C	-4.23698	11.73708	0
C	4.39473	12.01031	0
C	-2.88976	12.09586	0
C	3.41041	12.99765	0
C	12.89494	1.6243	0

C	17.02754	10.3552	0
C	14.06898	2.3968	0
C	15.77151	10.9857	0
C	14.00442	3.79205	0
C	14.59548	10.23216	0
C	12.76307	4.45013	0
C	14.64624	8.82808	0
C	11.58828	3.67892	0
C	15.90152	8.19628	0
C	11.6531	2.28368	0
C	17.07743	8.95004	0
C	12.69377	5.93028	0
C	13.39904	8.02799	0
N	11.49136	6.56142	0
N	13.45366	6.6711	0
S	-0.85481	20.66536	0
S	-5.02847	10.47522	0
C	12.97718	0.1433	0
C	18.26901	11.16692	0
N	1.72729	21.05171	0
N	-6.65411	12.5182	0
H	-3.33838	15.49314	0
H	0.69258	10.91049	0
H	-5.70649	14.79175	0
H	2.48406	9.21034	0
H	-2.13261	11.32228	0
H	3.70177	14.04015	0
H	15.04298	1.92425	0
H	15.69376	12.06547	0
H	14.93002	4.3536	0
H	13.64637	10.75297	0
H	10.61441	4.15212	0
H	15.97865	7.11629	0
H	10.72551	1.72773	0
H	18.02269	8.42469	0

Section S3 Characterization of TTI-COF, TTT-COF and Pd NPs@TTT-COF

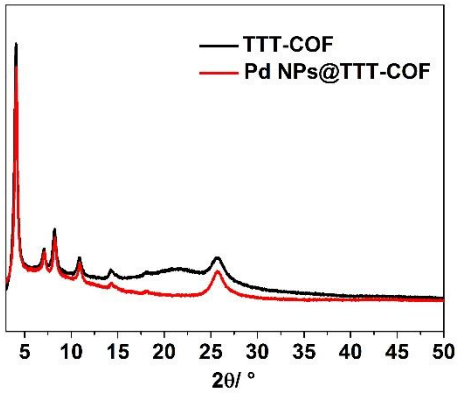

Figure S2. PXRD patterns of TTT-COF (black) and Pd NPs@TTT-COF (red).

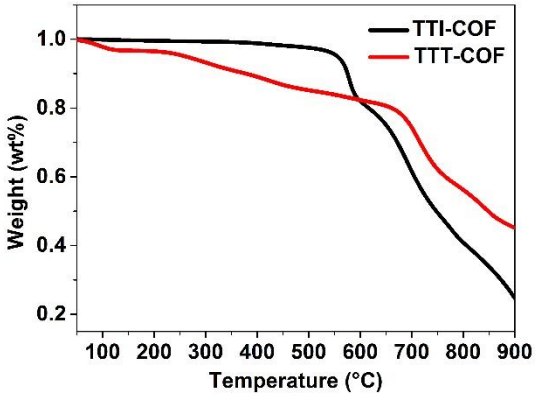

Figure S3. TGA curves of TTI-COF and TTT-COF under N_2 atmosphere.

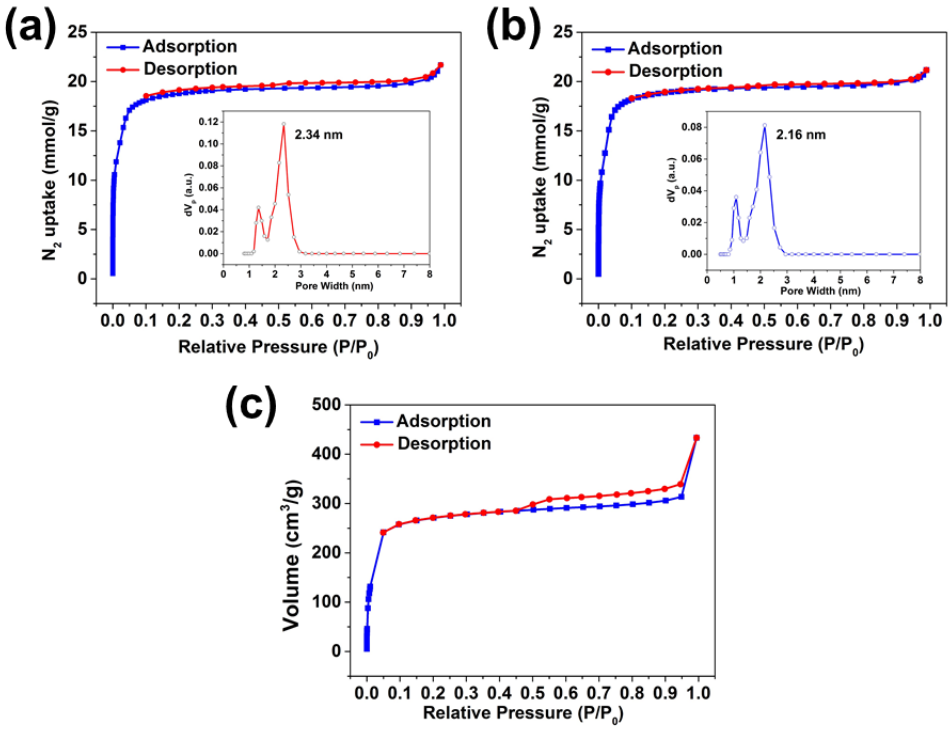

Figure S4. Nitrogen adsorption experiment. N_2 adsorption isotherm of TTI-COF (a), TTT-COF (b) and Pd NPs@TTT-COF (c). Inset: pore size distribution of TTI-COF and TTT-COF derived from NLDFT model.

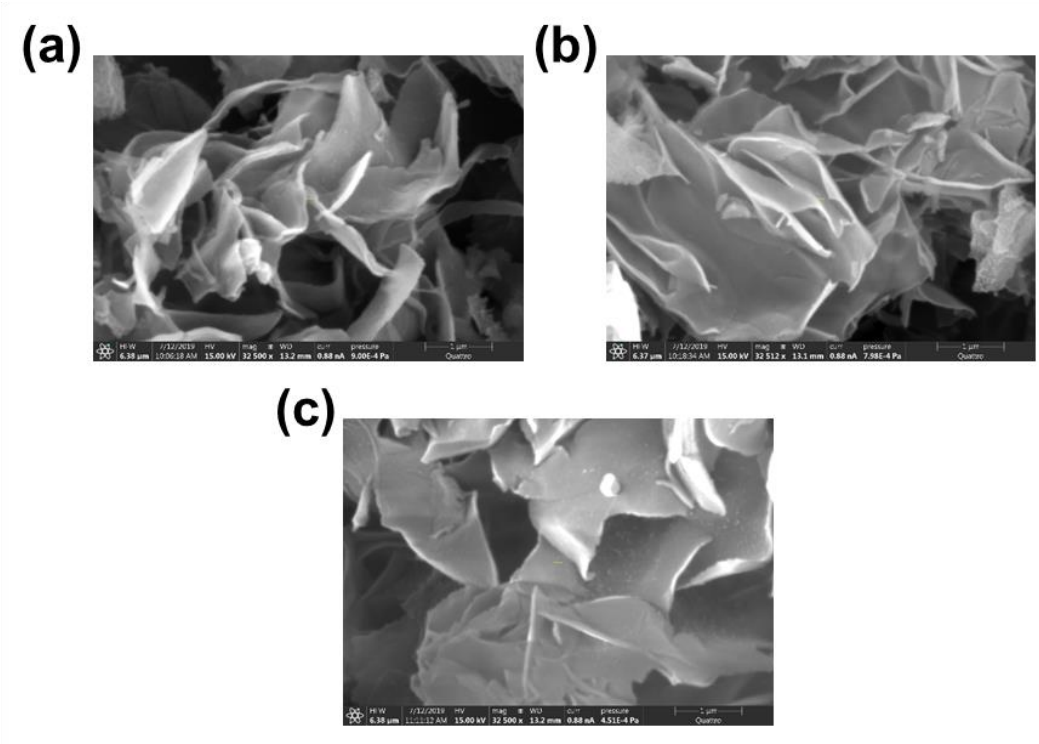

Figure S5. SEM images of TTI-COF (a), TTT-COF (b) and Pd NPs@TTT-COF (c).

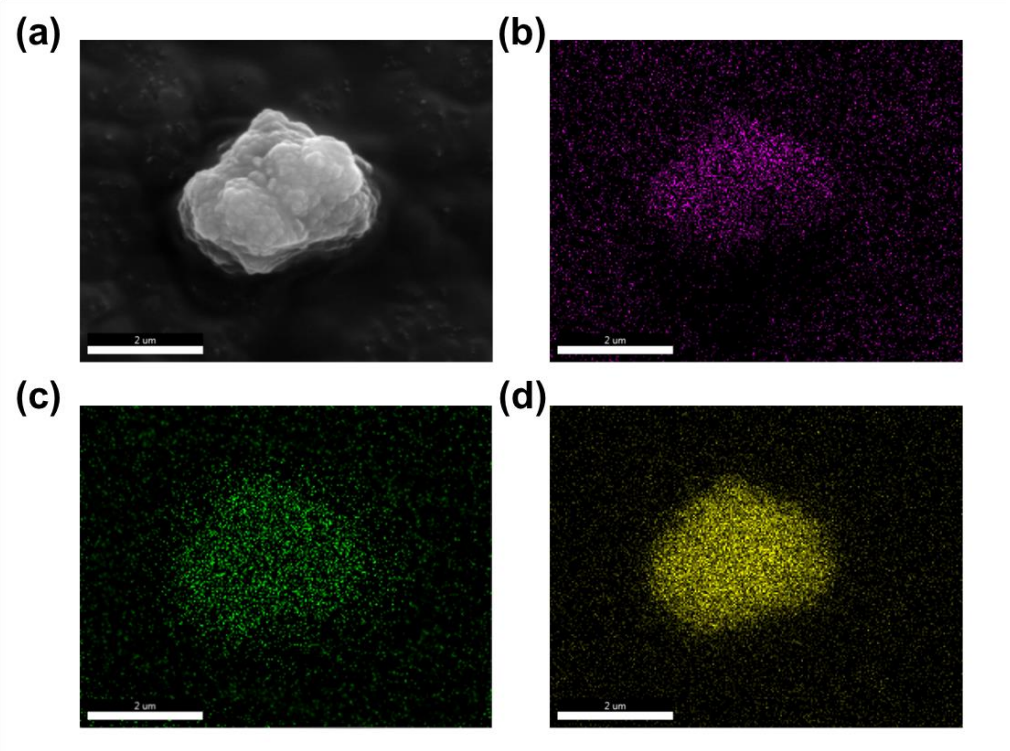

Figure S6. SEM image (a) and elemental mapping of nitrogen (b), palldium (c) and sulfur (d) in Pd NPs@TTT-COF.

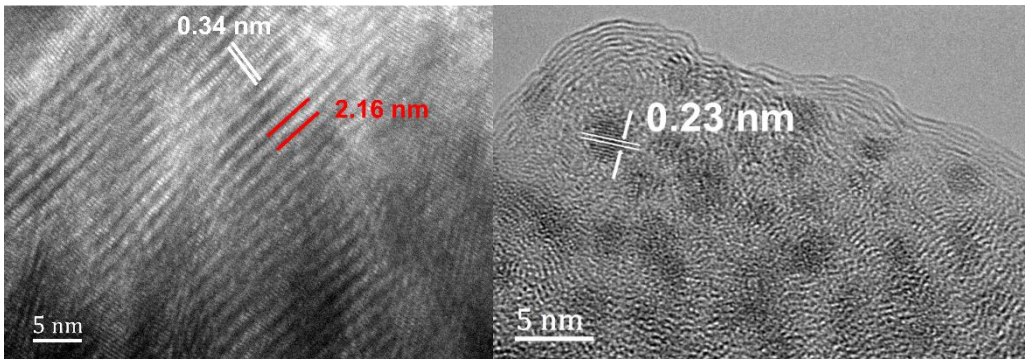

Figure S7. High-resolution TEM (HR-TEM) images of TTT-COF and Pd NPs@TTT-COF.

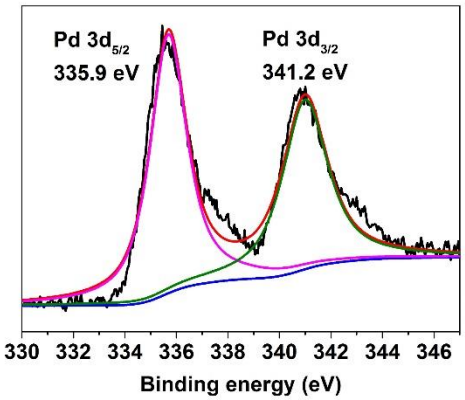

Figure S8. XPS Pd 3d spectrum of Pd NPs@TTT-COF.

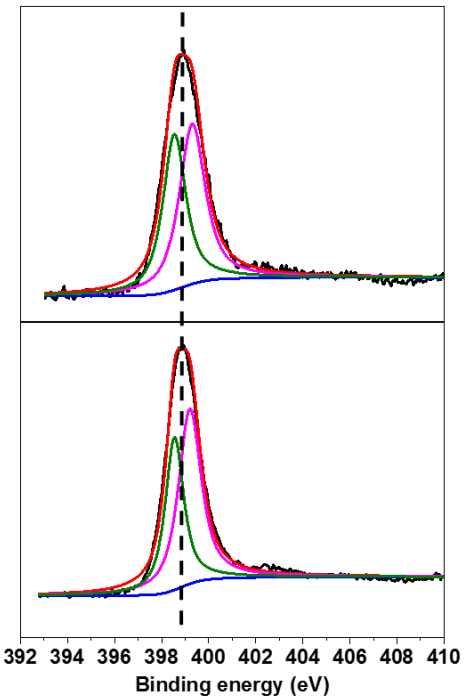

Figure S9. Comparison of N 1s spectrum before and after Pd NPs loading.

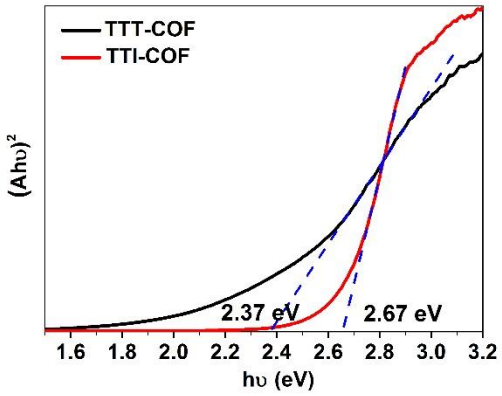

Figure S10. Tauc plot for absorption spectra obtained with Kubelka-Munk function and the linear fit for direct band gaps of TTI-COF and TTT-COF.

Section S3 Photocatalytic C-C Cross-Coupling Reactions by Pd NPs@TTT-COF

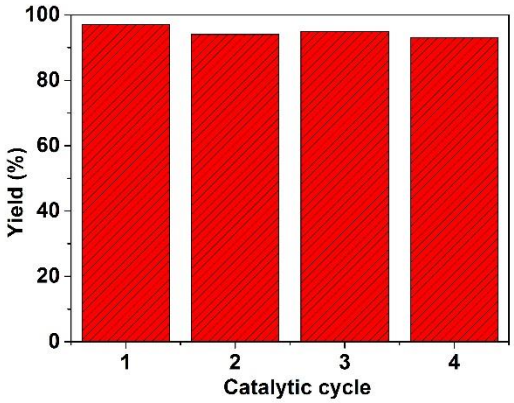

Figure S11. Investigation on reusability of Pd NPs@TTT-COF for photocatalytic model reaction.

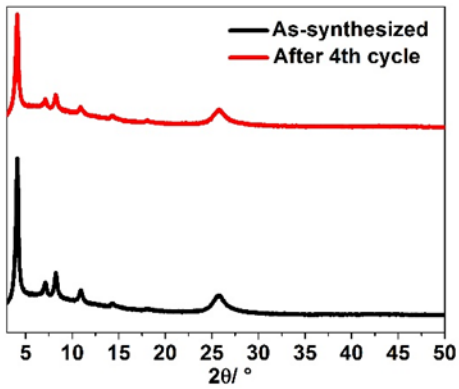

Figure S12. Comparison of PXRD patterns of Pd NPs@TTT-COF before and after 4th cycle.

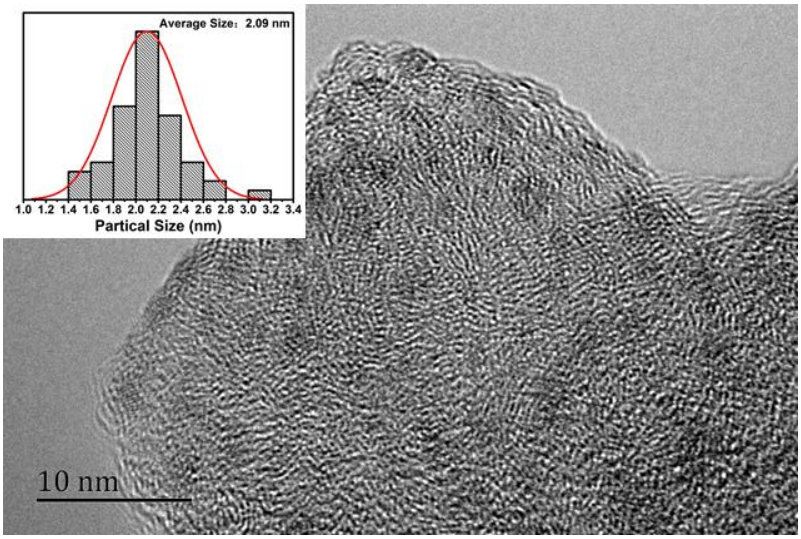

Figure S13. HR-TEM image of Pd NPs@TTT-COF after 4th photocatalytic cycle.

Table S3. Comparison of the photocatalytic activity of Pd NPs@TTT-COF for C-C cross-coupling reactions with other catalysts reported in literature.

Entry	Photocatalysts	Reation type (aryl iodides)	TOF/h^{-1}	Reference
1	Pd NPs@TTT-COF	Suzuki (iodotoluene)	344	this work
		Sonogashira (iodobenzene)	20.9	
		Heck (iodobenzene)	19.8	
		Stille (iodobenzene)	20.6	
2	B-BO_3/Pd NPs	Suzuki (iodobenzene)	88.7	[2]
3	m-CNR-Pd	Suzuki (iodobenzene)	51.6	[3]
4	Pd@NH2−Uio-66(Zr)	Suzuki (iodotoluene)	296.5	[4]
4	Au-Pd alloy on ZrO_2	Suzuki (iodotoluene)	17.1	[5]
		Sonogashira (iodotoluene)	4.1	[6]
		Stille (iodotoluene)	3.9	
5	Pd/CNC	Heck (iodobenzene)	13.1	[7]
6	Pd@TiO_2	Sonogashira (iodobenzene)	2.4	[8]
	Pd@Nb_2O_5		0.98	

Table S4. Control experiments for isomerization of stilbene.

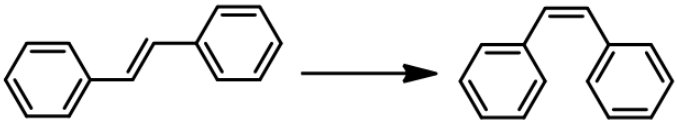

Entry	Photocatalysts	Light	Yield/%
1	-	√	**trace**
2	**Pd NPs@TTT-COF**	×	**0**
3	**Pd NPs@TTT-COF**	√	**58.3**
4	**TTT-COF**	√	**82.5**

Experiments conditions: 0.3 mmol *trans*-stilbene dissolved in 3 mL hot ethanol, 3 mL water added to the solution with sonicating 15 min. 5 mg photocatalysts was added and 300W Xe lamp was used as the light source for the 5 hours reaction. After the reaction, the solution was extracted with diethyl ether (5 mL×2) and analyzed by GC-MS.

Reference

[1] M. Papmeyer, C. A. Vuilleumier, G. M. Pavan, K. O. Zhurov, K. Severin, *Angew. Chem. Int. Ed.* **2016**, 55, 1685.

[2] Z. J. Wang, S. Ghasimi, K. Landfester, K. A. I. Zhang, *Chem. Mater.* **2015**, 27, 1921.

[3] X.-H. Li, M. Baar, S. Blechert, M. Antonietti, *Sci. Rep.* **2013**, 3.

[4] D. Sun, Z. Li, *J. Phy. Chem. C* **2016**, 120, 19744.

[5] S. Sarina, H. Zhu, E. Jaatinen, Q. Xiao, H. Liu, J. Jia, C. Chen, J. Zhao, *J. Am. Chem. Soc.* **2013**, 135, 5793.

[6] Q. Xiao, S. Sarina, A. Bo, J. Jia, H. Liu, D. P. Arnold, Y. Huang, H. Wu, H. Zhu, *ACS Catal.* **2014**, 4, 1725.

[7] X.-W. Guo, C.-H. Hao, C.-Y. Wang, S. Sarina, X.-N. Guo, X.-Y. Guo, *Catal. Sci. Tech.* **2016**, 6, 7738.

[8] A. Elhage, A. E. Lanterna, J. C. Scaiano, *ACS Sustainable Chem. Eng.* **2018**, 6, 1717.

NMR Spectra

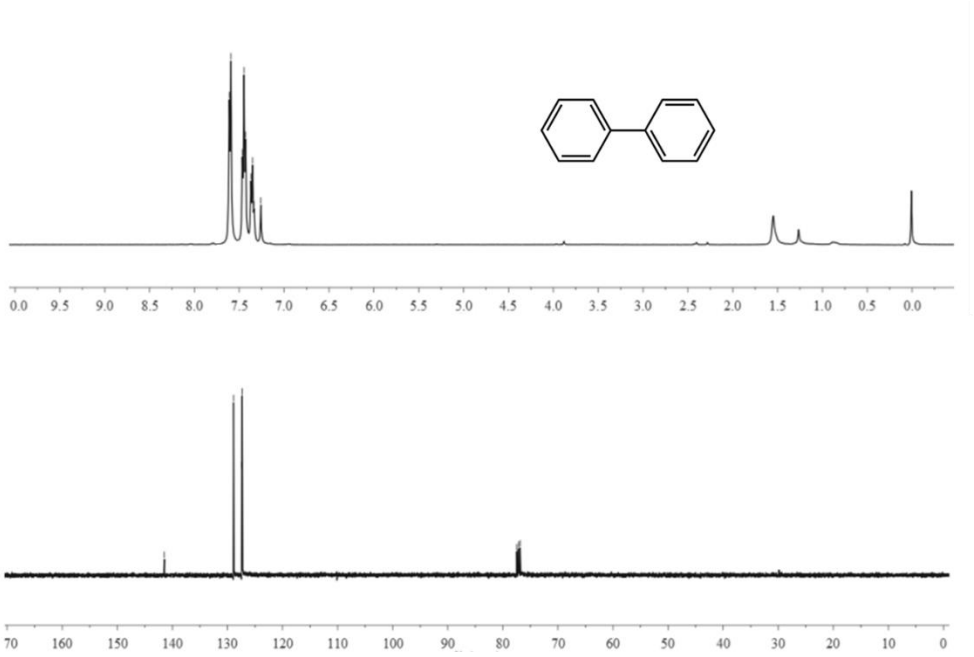

^{1}HNMR ($CDCl_3$, 400 MHz) δ: 7.26 (t, J＝7.6 Hz, 2H), 7.35 (t, J＝7.2 Hz, 4H), 7.49-7.52 (m, 4H);
^{13}C NMR ($CDCl_3$, 100 MHz) δ: 126.12, 126.20, 127.71, 140.20.

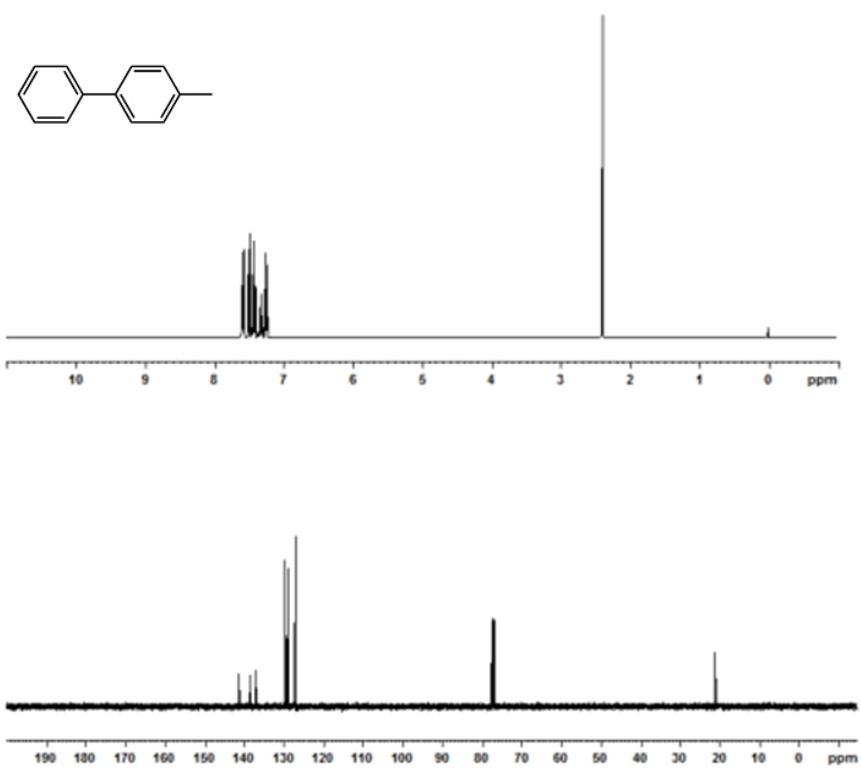

^{1}H NMR ($CDCl_3$, 400 MHz) δ: 2.30 (s, 3H), 7.15 (d, J＝8.0 Hz, 2H), 7.23 (t, J＝7.2 Hz, 1H), 7.33 (t, J＝7.6 Hz, 2H), 7.40 (d, J＝8.0 Hz, 2H), 7.49 (d, J＝8.4 Hz, 2H);
^{13}C NMR ($CDCl_3$, 100 MHz) δ: 20.04, 125.92, 125.94, 127.66, 128.43, 135.95, 137.32, 140.13.

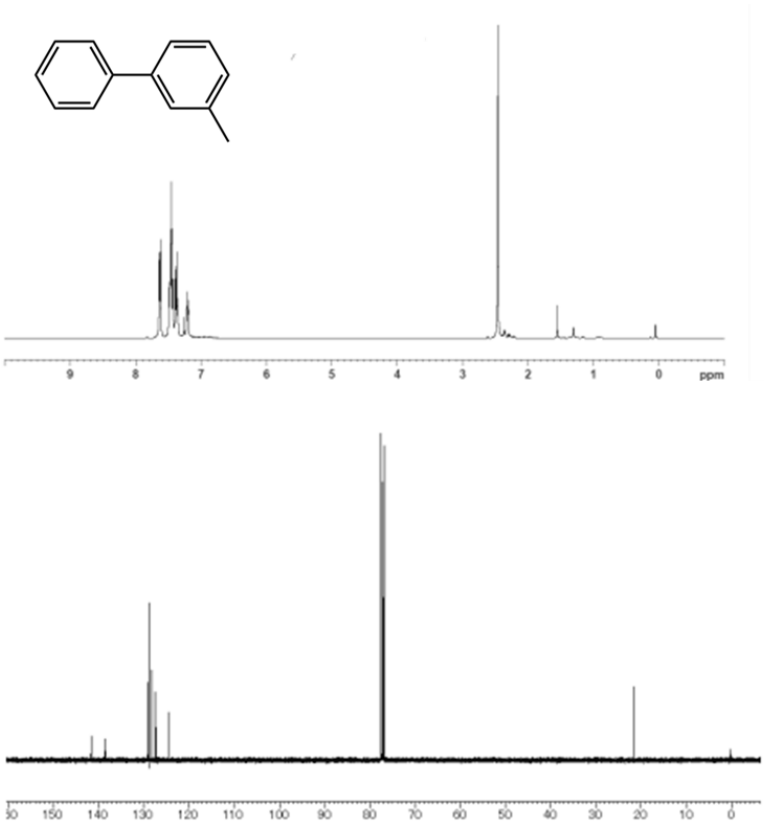

^{1}H NMR (400 MHz, $CDCl_3$) δ: 2.46 (s, 3H), 7.21 (d, J = 7.5, 1H), 7.37 (t, J = 8.4, 2H), 7.43-7.49 (m, 4H), 7.63 (d, J = 8.5, 2H);
^{13}C NMR (100 MHz, $CDCl_3$) δ: 21.5, 124.3, 127.2, 128.0, 128.7, 138.3, 141.2, 141.4.

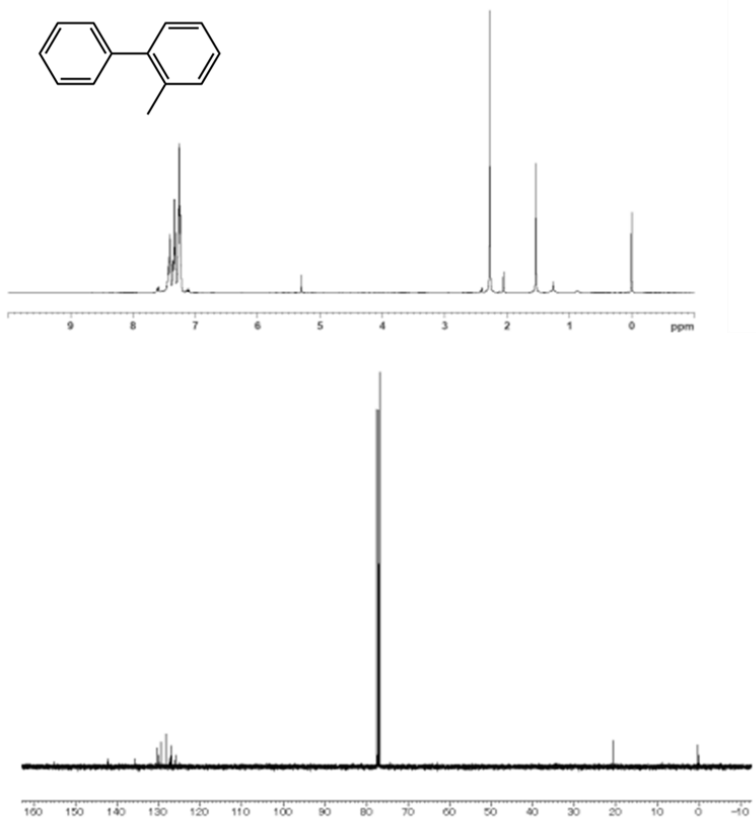

^{1}H NMR ($CDCl_3$, 400 MHz) δ: 2.26 (s, 3H), 7.21-7.25 (m, 4H), 7.29-7.32 (m, 3H), 7.38 (t, J＝7.4 Hz, 2H);
^{13}C NMR ($CDCl_3$, 100 MHz) δ: 20.44, 125.73, 126.72, 127.21, 128.03, 129.15, 129.76, 130.27, 135.28, 141.89, 141.92.

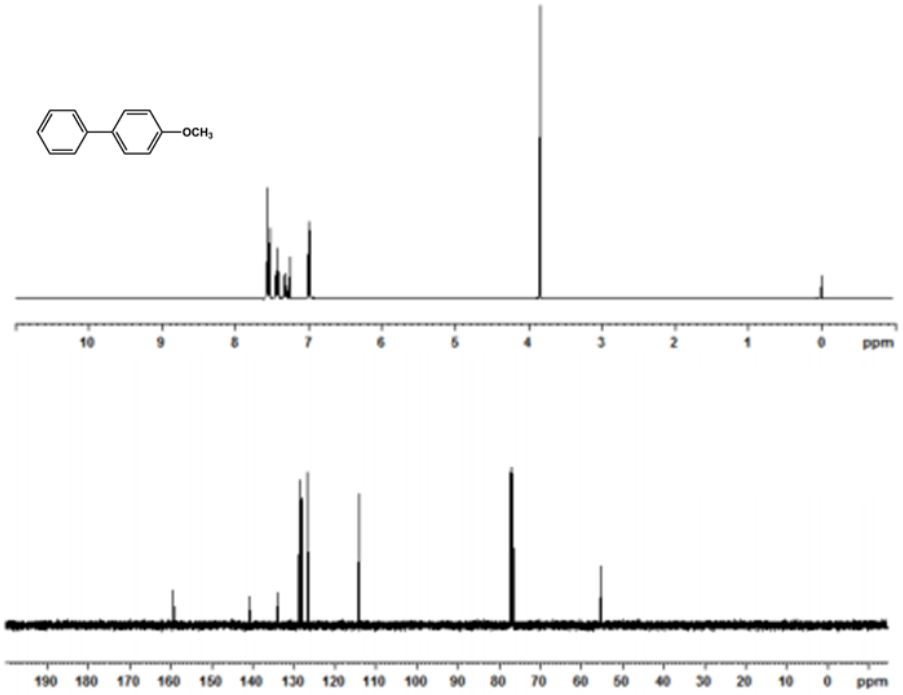

^{1}H NMR ($CDCl_3$, 400 MHz) δ: 3.85 (s, 3H), 6.98 (d, J＝9.2 Hz, 2H), 7.30 (t, J＝7.4 Hz, 1H), 7.42 (t, J＝7.6 Hz, 2H), 7.51-7.57 (m, 4H);
^{13}C NMR ($CDCl_3$, 100 MHz) δ: 55.35, 114.20, 126.65, 126.74, 128.15, 128.71, 133.79, 140.84, 159.15.

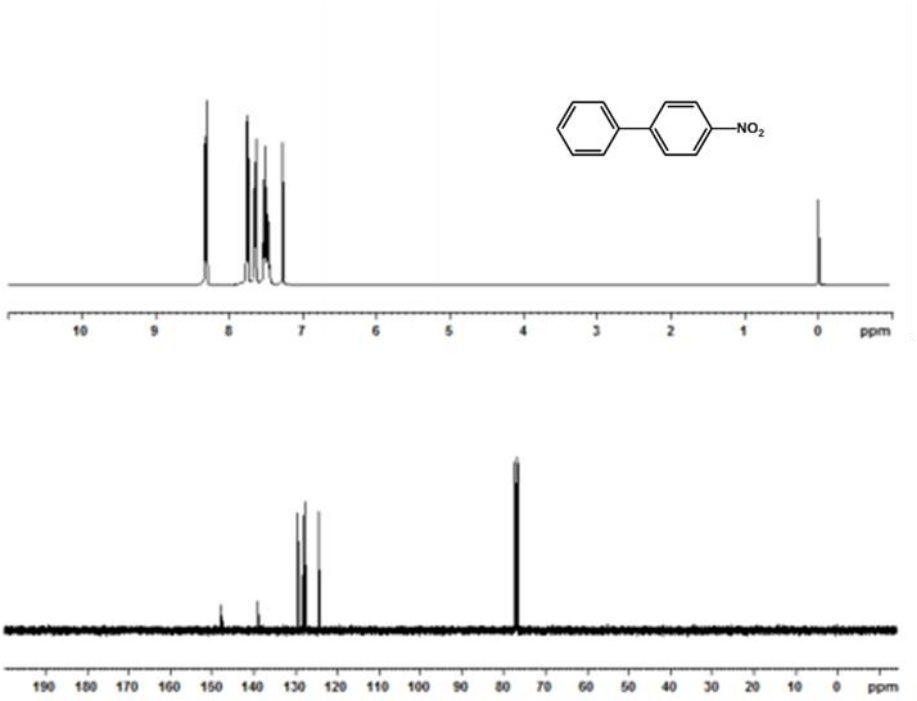

^{1}H NMR ($CDCl_3$, 400 MHz) δ: 7.43-7.47 (m, 3H), 7.62 (d, J＝6.8 Hz, 2H), 7.73 (d, J＝8.8 Hz, 2H), 8.29 (d, J＝8.8 Hz, 2H);
^{13}C NMR ($CDCl_3$, 100 MHz) δ: 124.09, 127.37, 127.78, 128.92, 129.15, 138.73, 147.04, 147.60.

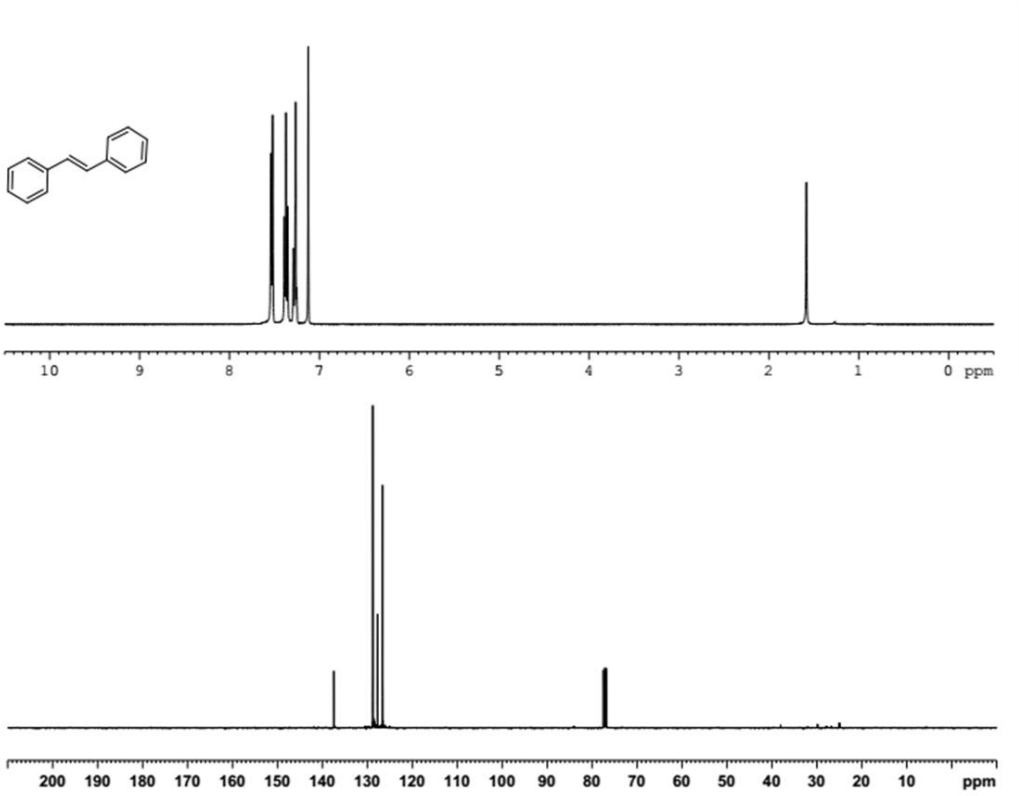

^{1}H NMR (400 MHz, $CDCl_3$) δ: 7.11 (s, 2H), 7.24-7.28 (m, 2H), 7.36 (t, J =7.6 Hz, 4H), 7.49-7.55 (m, 4H);
^{13}C NMR (100 MHz, $CDCl_3$) δ: 126.51, 127.62, 128.68, 128.69, 137.33.

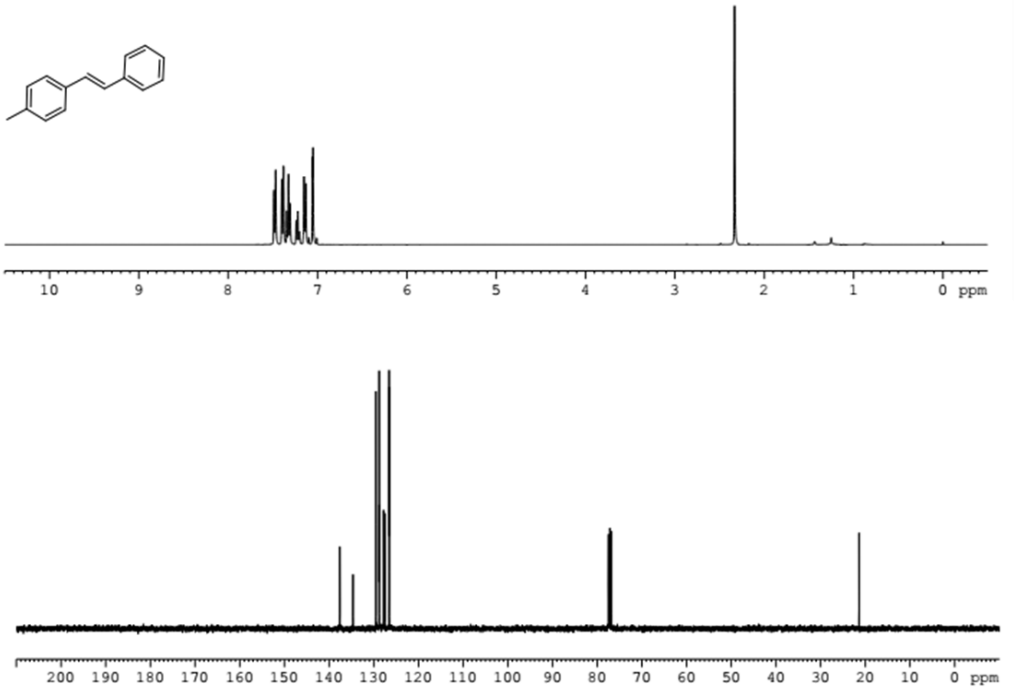

^{1}H NMR (400 MHz, $CDCl_3$) δ: 2.33 (s, 3H), 7.04 (d, J = 2.4 Hz, 1H), 7.12-7.21 (m, 2H), 7.21–7.23 (m, 1H), 7.30-7.34 (m, 2H), 7.38 (d, J = 8.0 Hz, 2H), 7.46-7.48 (m, 2H);
^{13}C NMR (100 MHz, $CDCl_3$) δ: 137.5, 137.4, 134.5, 129.3, 128.6, 128.5, 127.6, 127.3, 126.4, 126.3, 21.2.

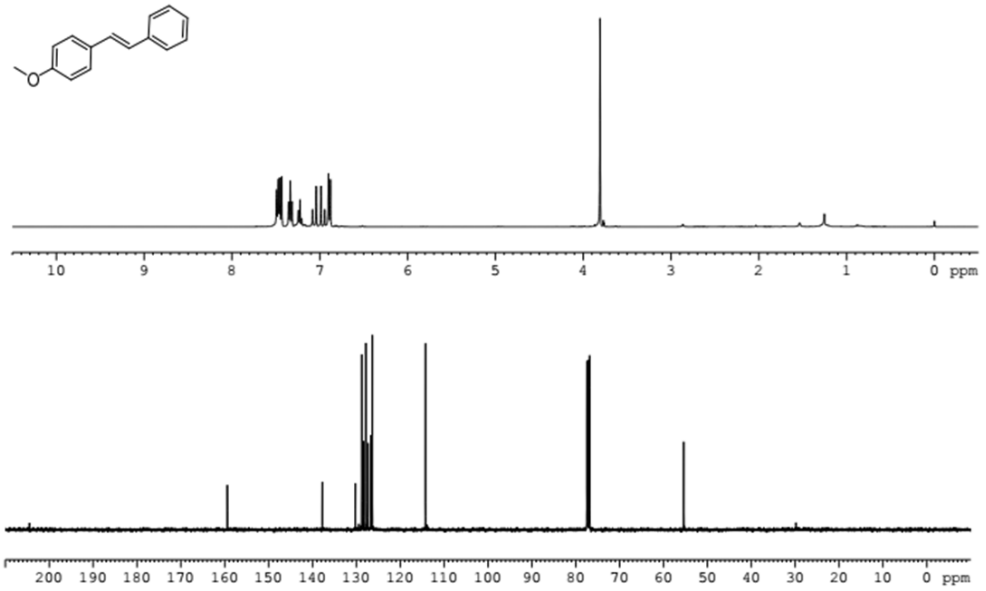

^{1}H NMR (400 MHz, $CDCl_3$) δ: 3.86 (s, 3H), 6.93 (d, J = 11.7 Hz, 2H), 7.05 (m, 2H), 7.21-7.32(m, 1H), 7.37 (t, J = 7.6 Hz, 2H), 7.50 (m, 4H);
^{13}C NMR (100 MHz, $CDCl_3$) δ: 55.33, 114.1, 126.25, 126.62, 127.25, 127.71, 128.21, 128.64, 130.19, 137.65, 159.30.

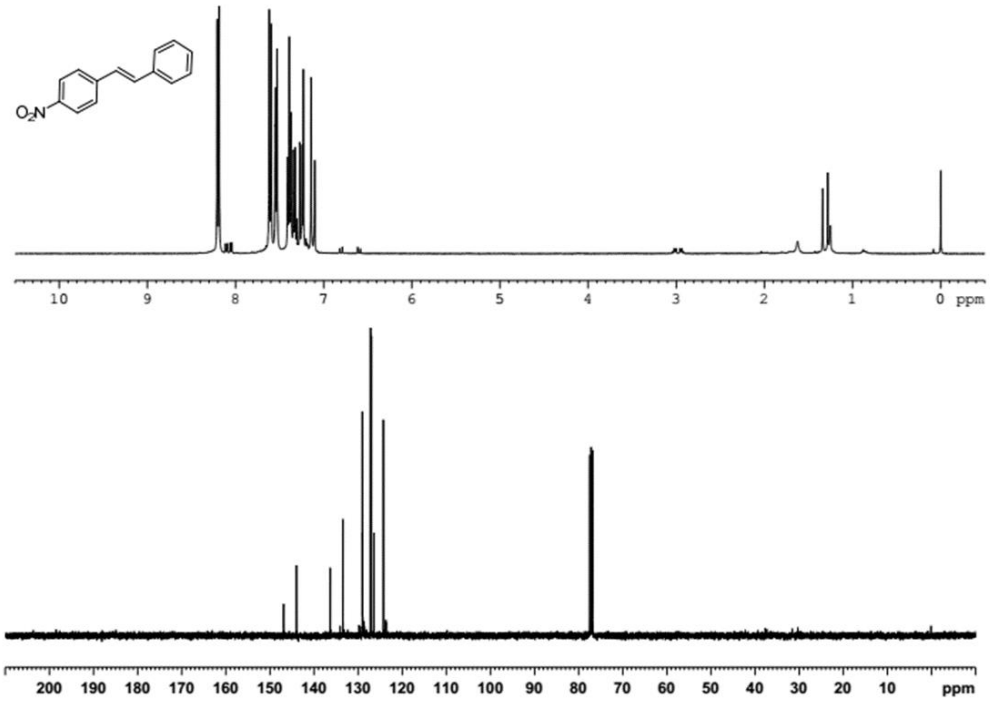

^{1}H NMR (400MHz, $CDCl_3$) δ: 7.17 (d, J = 16.3 Hz, 1H), 7.30 (d, J = 16.3 Hz, 1H), 7.36 (t, J = 7.3 Hz, 1H)， 7.43 (t, J = 7.4 Hz, 2H), 7.58 (d, J = 7.2 Hz, 2H), 7.66 (d, J = 8.8 Hz, 2H), 8.25 (d, J = 8.8 Hz, 2H);
^{13}C NMR (100 MHz, $CDCl_3$) δ: 124.15, 126.30, 126.86, 127.02, 128.84, 128.90, 133.32, 136.19, 143.88, 146.80.

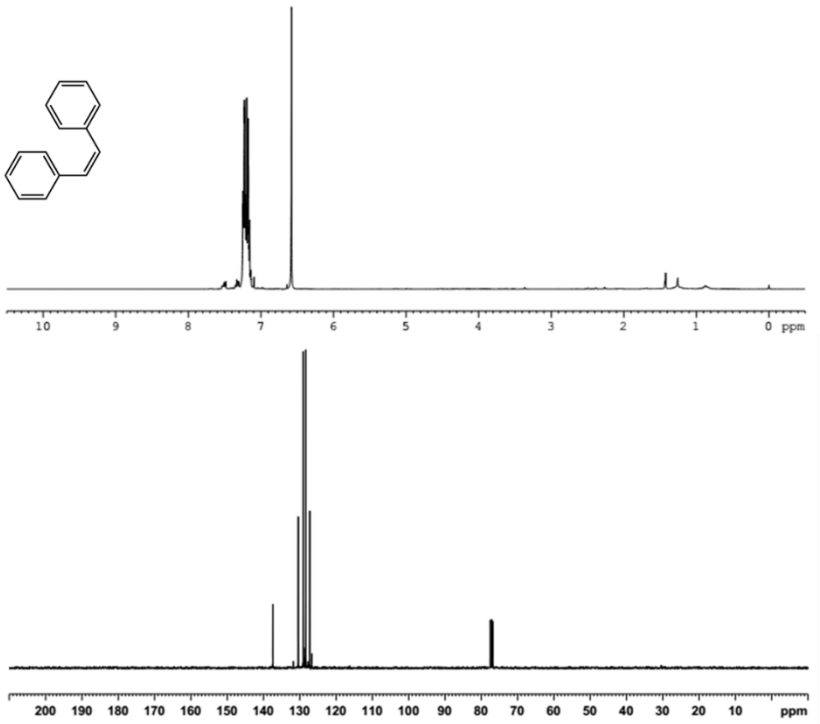

^{1}H NMR (400 MHz, $CDCl_3$) δ: 6.56 (s, 2H), 7.11-7.22 (m, 10H);
^{13}C NMR (100 MHz, $CDCl_3$) δ: 127.0, 128.2, 128.8, 130.2, 137.1.

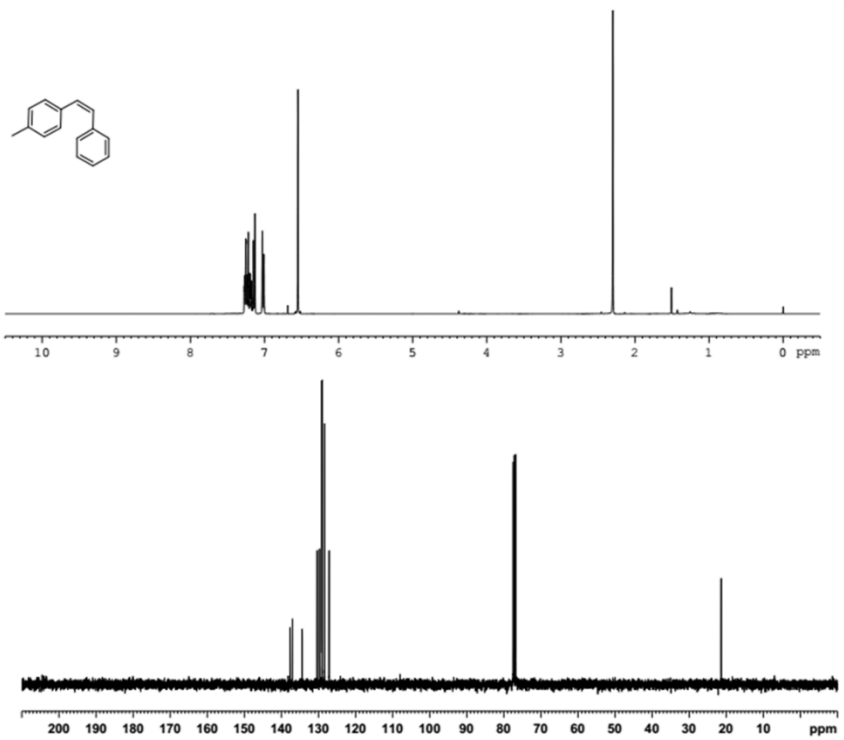

^{1}H NMR (400 MHz, $CDCl_3$) δ: 2.28 (s, 3H), 6.53 (s, 2H), 7.00 (d, J = 7.6 Hz, 2H), 7.12-7.26 (m, 7H);
^{13}C NMR (100 MHz, $CDCl_3$) δ: 21.2, 126.9, 128.2, 128.74, 128.79, 128.86, 129.5, 130.1, 134.2, 136.8, 137.4.

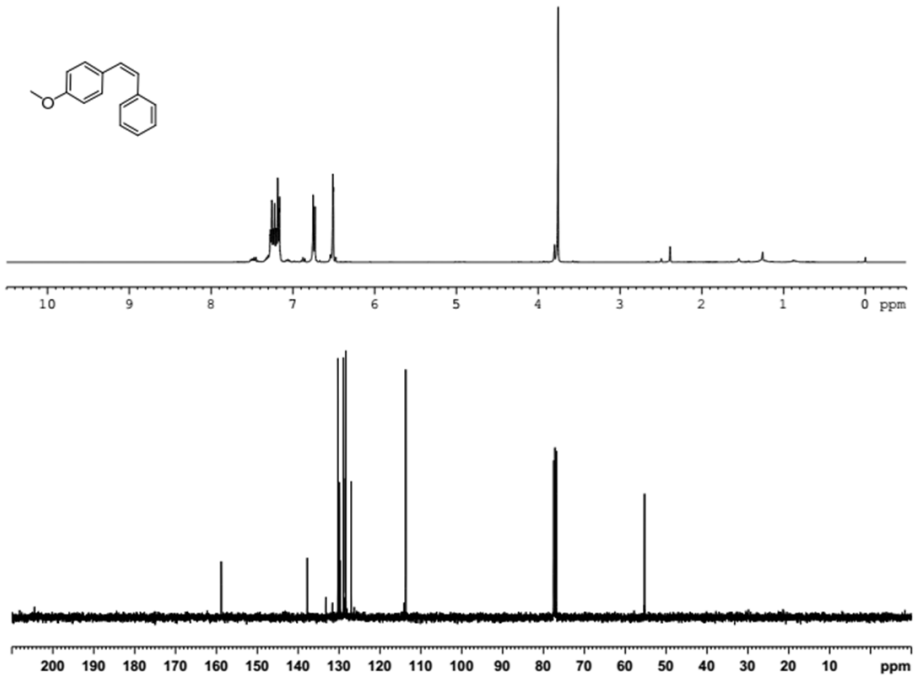

^{1}H NMR (400 MHz, $CDCl_3$) δ: 3.76 (s, 3H), 6.51 (d, J = 2.0 Hz, 2H), 6.51-6.77 (m, 2H), 7.09-7.28 (m, 7H);
^{13}C NMR (100 MHz, $CDCl_3$) δ: 55.1, 113.5, 126.8, 128.2, 128.7, 128.8, 129.6, 129.7,

130.1, 137.6, 158.6.

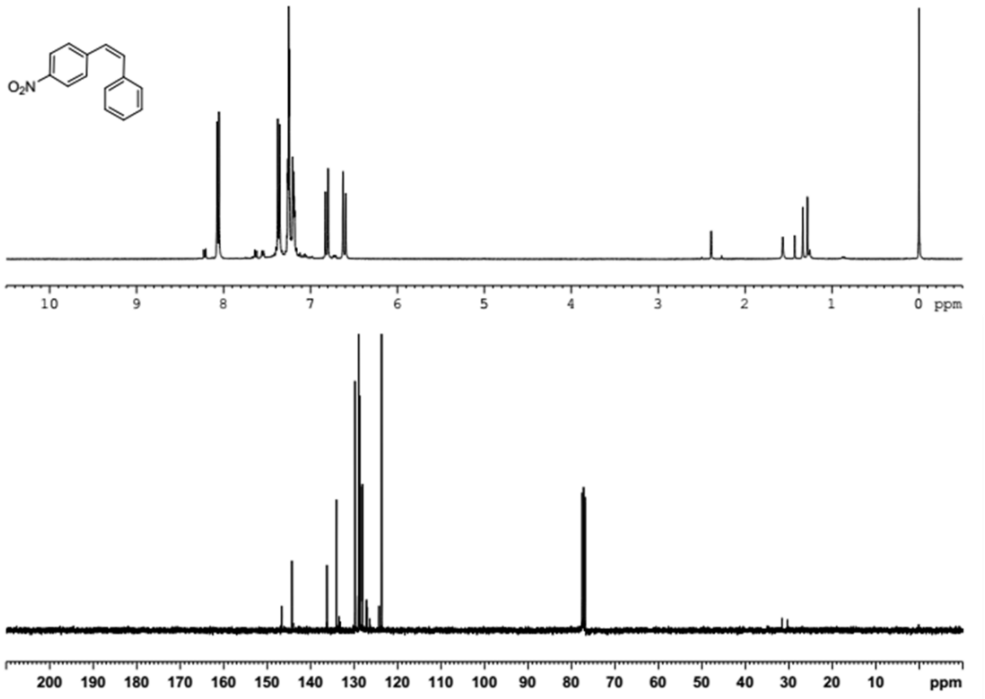

^{1}H NMR (400 MHz, $CDCl_3$) δ: 6.60 (d, J = 12.4 Hz, 2H), 6.81 (d, J = 12 Hz, 2H), 7.18–7.21 (m, 2H), 7.24 –7.26 m, 3H), 7.36 (d, J = 8.8 Hz, 2H), 8.06 (d, J = 8.8 Hz, 2H).
^{13}C NMR (100 MHz, $CDCl_3$) δ: 123.64, 128.04, 128.09, 128.65, 128.88, 129.74, 134.03, 136.21, 144.25, 146.62.

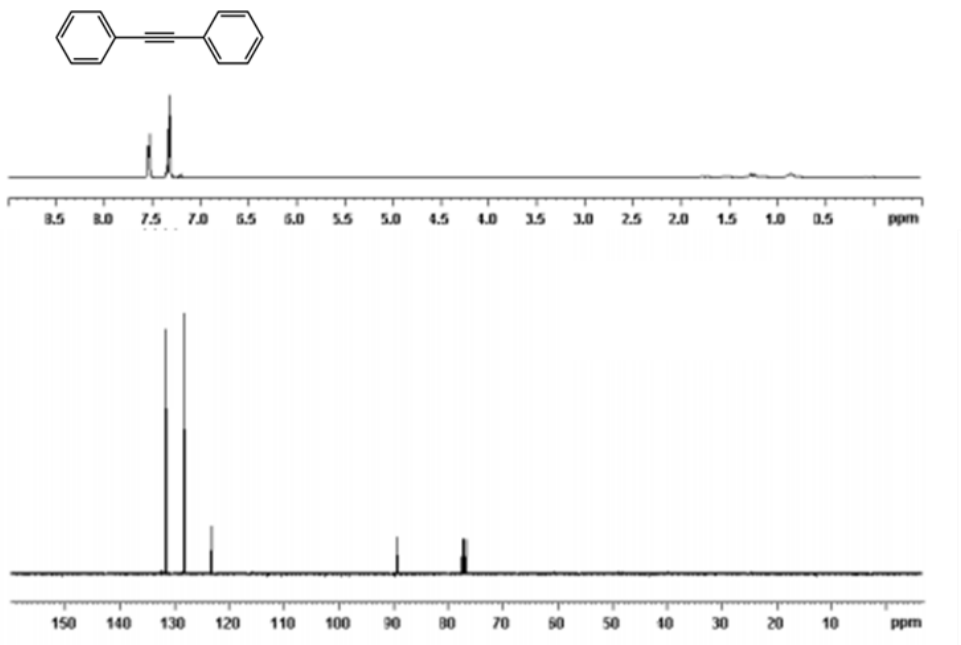

^{1}H NMR (400 MHz, $CDCl_3$) δ: 7.31–7.33 (m, 6H), 7.52–7.54 (m, 4H);

^{13}C NMR (100 MHz, $CDCl_3$) δ: 89.4, 123.2, 128.2, 128.3, 131.6.

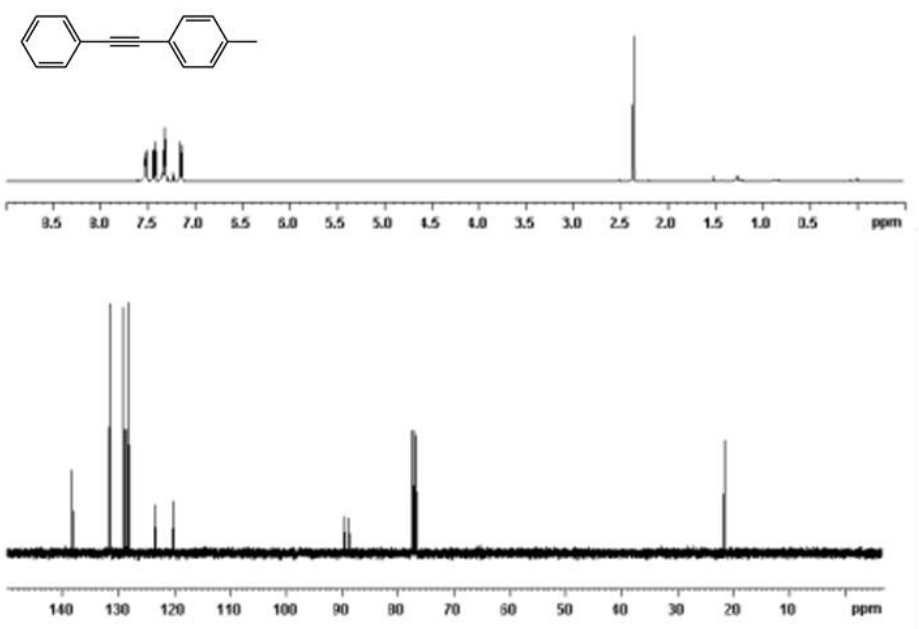

^{1}H NMR (400 MHz, $CDCl_3$) δ: 2.35 (s, 3H), 7.14 (d, J = 8.0 Hz, 2H), 7.30–7.34 (m, 3H), 7.42 (d, J = 8.0 Hz, 2H), 7.51–7.53 (m, 2H);
^{13}C NMR (100 MHz, $CDCl_3$) δ: 21.5, 88.7, 89.5, 120.2, 123.4, 128.0, 128.3, 129.1, 131.4, 131.5, 138.3.

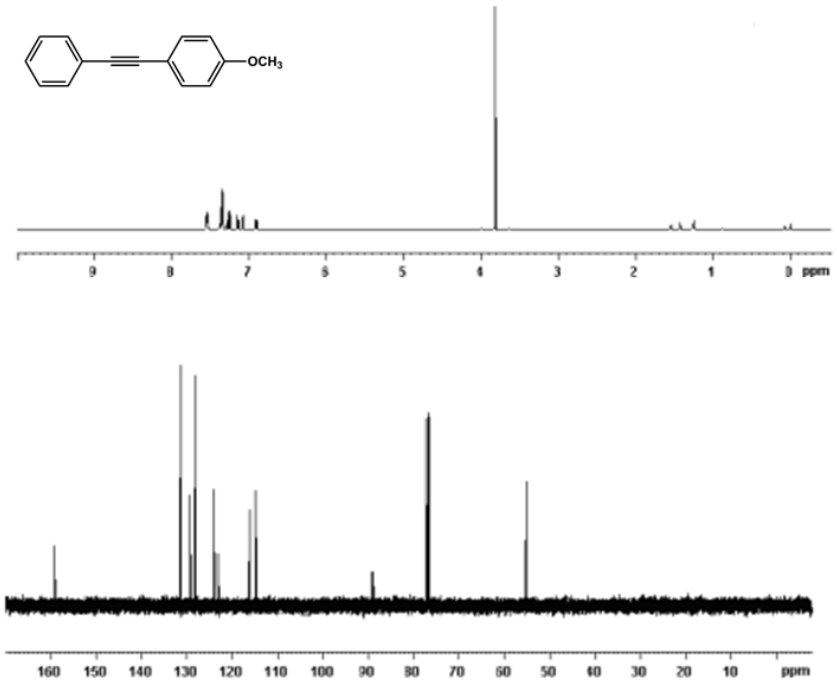

^{1}H NMR (400 MHz, $CDCl_3$) δ: 3.82 (s, 3H), 6.88–6.90 (m, 1H), 7.06 (t, J = 1.2 Hz,

1H), 7.12–7.14 (m, 1H), 7.23–7.27 (m, 1H), 7.33–7.35 (m, 3H), 7.52–7.55 (m, 2H),;
^{13}C NMR (100 MHz, $CDCl_3$) δ: 159.3, 131.6, 129.4, 128.3, 124.2, 123.2, 116.3, 114.9, 89.3, 89.2, 55.3.

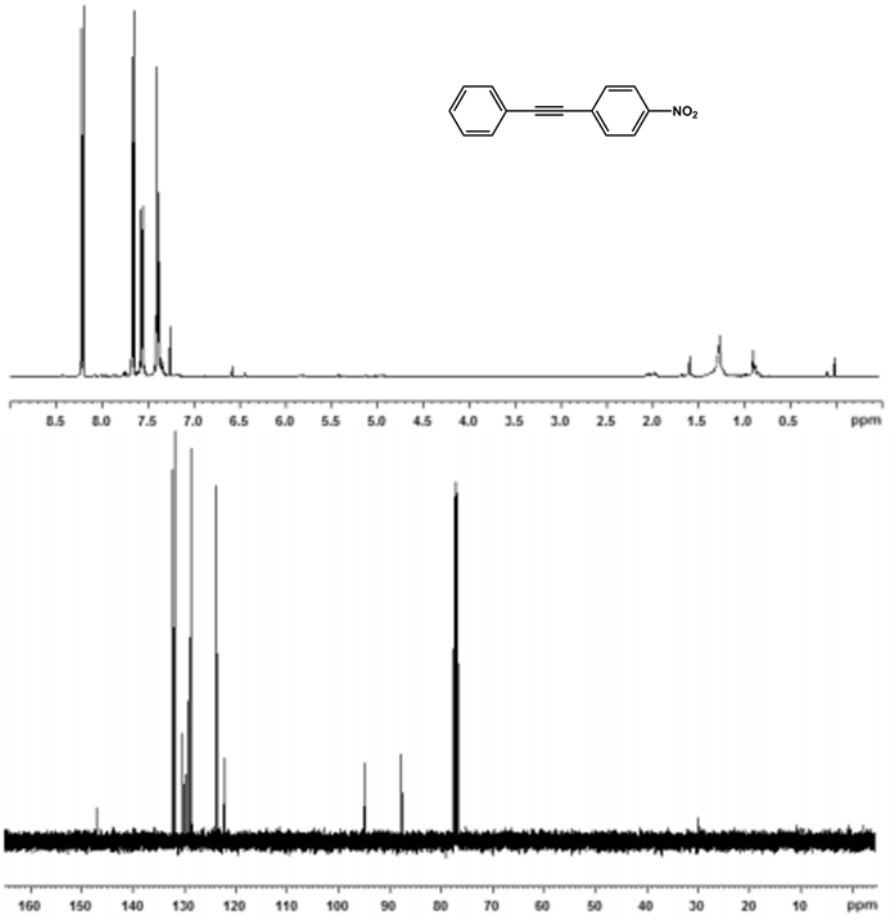

^{1}H NMR (400 MHz, $CDCl_3$) δ: 7.38–7.41 (m, 3H), 7.55–7.57 (m, 2H), 7.65 (d, J = 8.4 Hz, 2H), 8.21 (d, J = 8.4 Hz, 2H);
^{13}C NMR (100 MHz, $CDCl_3$) δ: 87.5, 94.7, 122.1, 123.6, 128.5, 129.2, 130.2, 131.8, 132.2, 146.9.